

# Extension of a System Level Tool for Component Level Analysis

Alok Majumdar  
NASA Marshall Space Flight Center  
MSFC, AL

Paul Schallhorn  
Sverdrup Technology, Inc.  
Edwards, CA

*This paper presents an extension of a numerical algorithm for network flow analysis code to perform multi-dimensional flow calculation. The one dimensional momentum equation in network flow analysis code has been extended to include momentum transport due to shear stress and transverse component of velocity. Both laminar and turbulent flows are considered. Turbulence is represented by Prandtl's mixing length hypothesis. Three classical examples (Poiseuille flow, Couette flow and shear driven flow in a rectangular cavity) are presented as benchmark for the verification of the numerical scheme.*

## 1.0 Introduction

Traditionally, fluid network codes have been used for system level analyses, whereas Navier-Stokes(NS) codes have been used for component level analyses. Until recently, most attempts to merge the two methodologies have come from the NS side (i.e. using a NS code to perform a system level analysis). This approach brings the enormous overhead associated with such a code. The current approach, on the other hand, begins from the fluid network side. The system level code utilized in the current study is the Generalized Fluid System Simulation Program (GFSSP) [1].

The Generalized Fluid System Simulation Program was developed for the purpose of calculating pressure and flow distribution in a complex flow network associated with secondary flow in a liquid rocket engine turbopump. The code was developed to be a general purpose flow network solver so that generic networks could be modeled. A given fluid system is discretized into the nodes and branches. This practice is conceptually similar to the "staggered grid" practice of SIMPLE algorithm of Patankar & Spalding[2]. GFSSP employs a finite volume formulation of mass, momentum, and energy conservation equations in conjunction with the thermodynamic equations of state for real fluids. Mass, energy and specie conservation equations are solved at the nodes; the momentum conservation equations are solved in the branches. The system of equations describing the fluid network is solved by a hybrid numerical method that is a combination of the Newton-Raphson and successive substitution methods. Eighteen different resistance/source options are provided for modeling momentum sources or sinks in the branches. Two thermodynamic property programs, GASP-WASP[3,4] and GASPAK[5]

are integrated with the code to provide thermodynamic and thermophysical properties of real fluid. GFSSP's system level capability has been extensively verified by comparing with test data [6-10].

## 2.0 Unstructured Finite Volume Grid

The unstructured finite volume grid network for GFSSP is shown in Figure 1, which shows connectivity of five nodes with four branches. In this figure node-i is connected with four neighboring nodes ( $j = 1$  to  $4$ ). In structured coordinate systems the number of neighboring nodes are restricted to 2, 4 and 6 for one, two and three dimensional systems respectively. On the other hand for an unstructured system, there is no such restriction on the number of neighboring nodes. The index  $k$  represents fluid species.

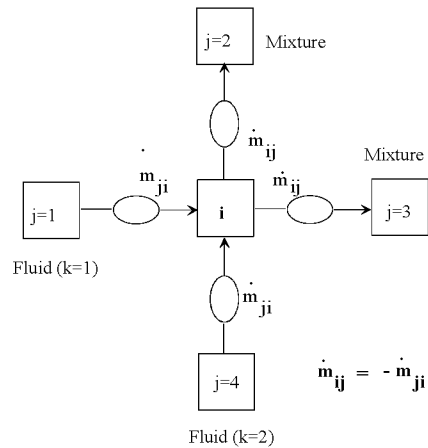


Figure 1: Schematic of Nodes and Branches for an Unstructured Finite Volume Grid

## 3.0 Conservation Equations

### 3.1 Mass Conservation Equation

The mass conservation equation for the  $i^{\text{th}}$  node can be represented by:

$$\sum_{j=1}^n \dot{m}_{ij} = 0 \quad (1)$$

Equation 1 implies that the net mass flow from a given node must equate to zero. In other words, the total mass flow rate into a node is equal to the total mass flow rate out of the node.

### 3.2 Momentum Conservation Equation

The one dimensional form of momentum equation for every branch takes the following form:

$$\begin{aligned} \frac{m_{ij, dot}}{g_c} (u_i - u_u) &= (p_i - p_j) A + \frac{\rho g V \cos \theta}{g_c} \\ - K_f m_{ij, dot} |m_{ij, dot}| A &+ \frac{\rho K_{rot}^2 \omega^2 A}{2 g_c} (r_j^2 - r_i^2) + S \end{aligned} \quad (2)$$

Equation 2 represents the balance of fluid forces acting on a given branch. Inertia, pressure, gravity, friction and centrifugal forces are considered in the conservation equation. In addition to five forces, a source term S has been provided in the equation to input pump characteristics or to input power to pump in a given branch. If a pump is located in a given branch, all other forces except pressure are set to zero. The source term S is set to zero in all other cases. Figure 2 shows the schematic of a branch control volume.

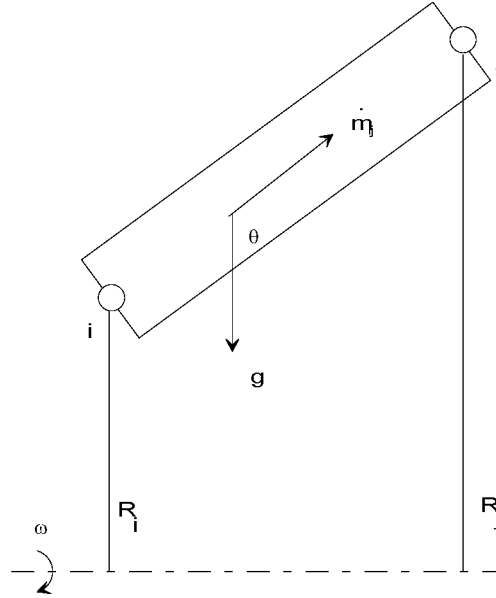


Figure 2: Schematic of a Branch Control Volume Showing the Gravity and Rotation

Multi-dimensional conservation equations must account for the transport of mass, momentum and energy into and out of the control volume from all directions in space. Mass conservation equations (Equation 1) can account for such transport because each internal node can be connected with multiple neighboring nodes located in space in any arbitrary location (Figure 1). On the other hand, the momentum conservation equation (Equation 2) is one dimensional. Multi-dimensional momentum transport can be accounted for by incorporating two additional terms in the momentum equation. These

terms include: a) momentum transport due to shear, and b) momentum transport due to the transverse component of velocity.

These two terms can be identified in the two-dimensional steady state Navier-Stokes equation which can be expressed as:

$$\begin{aligned} \rho \left( u \frac{\partial u}{\partial x} + v \frac{\partial u}{\partial y} \right) &= \frac{\partial(\rho uu)}{\partial x} + \frac{\partial(\rho vu)}{\partial y} \\ &= -\frac{\partial p}{\partial x} + \rho g_x + \mu \left( \frac{\partial^2 u}{\partial x^2} + \frac{\partial^2 u}{\partial y^2} \right) \end{aligned} \quad (3)$$

The first term on the left hand side of Equation 3 corresponds to the current inertia term described in Equation 2. The second term on the left hand side of Equation 3 corresponds to the transverse momentum exchange. The first term on the right hand side corresponds to the pressure term in Equation 2. The second term on the right hand side of Equation 3 corresponds to the gravity term. The third term on the right hand side of the equation is negligible (based on an order of magnitude argument). The fourth term on the right hand side represents momentum transport due to shear. The next two subsections describe the implementation of shear and transverse momentum transport into the momentum equation of GFSSP. A more detailed description of the implementation of these terms for laminar flow is detailed by Schallhorn [11].

### 3.3 Momentum Transport Due to Shear

#### 3.3.1 Laminar Flow

Begin by examining the shear term (fourth term) of the Navier-Stokes Equation in more detail. First, consider the shear as a force instead of a force per unit volume by multiplying the volume by the shear term.

$$\mu \frac{\partial^2 u}{\partial y^2} V \approx \mu \frac{\Delta u}{(\Delta y)^2} (\Delta x)(\Delta y)(\Delta z) = \mu \frac{\Delta u}{\Delta y} \Delta x \Delta z = \mu \frac{\Delta u}{\Delta y} A_{\text{shear}} \quad (4)$$

Figure 3 represents a set of nodes and branches for which shear forces are exchanged. Let branch 12 represent the branch for which the shear force is to be calculated. Branches N12 and S12 represent the parallel branches which will be used to calculate the shear force on branch 12. Let YS be the distance between branches 12 and S12, and let YN be the distance between branches 12 and N12. Let AS be the shearing area between branches 12 and S12, while AN is the shearing area between branches 12 and N12.

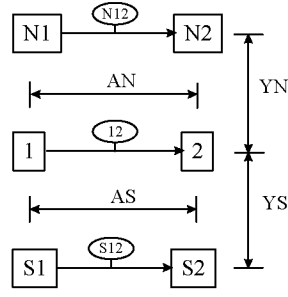


**Figure 3: Branch and Node Schematic for Shear Exchange**

A differencing scheme that can account for non-orthogonality in node structure was used. Equation 5 represents the shear term for branch 12. The angle  $\theta$  represents the angle that adjacent branches make with respect to the referenced branch.

$$\mu \frac{\partial u}{\partial y} A_{\text{Branch12shear}} \approx \left[ \left( \mu \frac{u_{N12} \cos \theta_{N12} - u_{12}}{Y_N} AN \right) + \left( \mu \frac{u_{12} - u_{S12} \cos \theta_{S12}}{Y_S} AS \right) \right] \quad (5)$$

Equation 5 can be generalized to n-number of parallel branches at any position around branch 12 as shown in Equation 6.

$$\mu \frac{\partial u}{\partial y} A_{\text{Branch12shear}} \approx \sum_{i=1}^n \left( \mu \frac{u_{i12} \cos \theta_{i12} - u_{12}}{Y_i} A_i \right) \quad (6)$$

Where the summation subscript  $i$  represents the  $i^{\text{th}}$  parallel branch to branch 12.

Next, the shear interaction with a neighboring parallel wall should be addressed. Suppose that adjacent to branch 12 is a wall that is approximately parallel to the branch. The angle  $\theta_{\text{wall}}$  represents the angle between branch 12 and the wall. The wall has a velocity  $u_{\text{wall}}$ . The distance between the centerline of branch 12 and the wall is  $y_{\text{wall}}$  and the shear area is  $A_{\text{wall}}$ . The expression for the shear effect of the wall on branch 12 is given in Equation 7.

$$\mu \frac{\partial u}{\partial y} A \Big|_{\text{Branch12-wall}_{\text{shear}}} \approx \mu \frac{u_{\text{wall}} \cos \theta_{\text{wall}} - u_{12}}{y_{\text{wall}}} A_{\text{wall}} \quad (7)$$

If there were multiple walls adjacent to branch 12, then Equation 7 could be generalized into Equation 8.

$$\mu \frac{\partial u}{\partial y} A \Big|_{\text{Branch12-wall}_{\text{shear}}} \approx \sum_{i=1}^n \left( \mu \frac{u_{\text{wall}_i} \cos \theta_{\text{wall}_i} - u_{12}}{y_{\text{wall}_i}} A_{\text{wall}_i} \right) \quad (8)$$

Finally, combining the adjacent branch and the wall shear equations into one generalized equation for the  $i^{\text{th}}$  branch for which shear is to be calculated. Equation 9 represents the actual laminar shear formulation incorporated into GFSSP, where  $i$  is the current branch,  $np_i$  is the number of parallel branches to branch  $i$ , and  $ns_i$  is the number of parallel solid walls to branch  $i$ .

$$\mu \frac{\partial u}{\partial y} A_{\text{Branch } i \text{ shear}} \approx \sum_{j=1}^{np_i} \left( \mu \frac{u_{ij} \cos \theta_{ij} - u_i}{Y_{ij}} A_{ij} \right) + \sum_{k=1}^{ns_i} \left( \mu \frac{u_{\text{wall } ik} \cos \theta_{\text{wall } ik} - u_i}{y_{\text{wall } ik}} A_{ik} \right) \quad (9)$$

### 3.3.2 Turbulent Flow

To model shear stress in a turbulent flow, a turbulence model must be employed. Separate methods must be used to model the interaction between adjacent branches and between branches and adjacent walls. The following two sections provide the details for the modeling of these interactions.

#### 3.3.2.1 Branch-Branch Interaction

Turbulent shear stress interaction between a branch and one of its neighboring branches is modeled using a modified form of the Mixing Length algebraic model proposed by Prandtl (see reference 5 for a description of Prandtl Mixing Length model). Referring to Figure 3 again, shear interaction between branch 12 and branch N12 is determined by their relative mean velocities, the shear area (AN) and the distance between the two branches (YN). In the original mixing length turbulence model proposed by Prandtl, viscosity (beginning with Equation 3) is replaced by an effective viscosity. This effective viscosity is defined as the sum of the viscosity and a “turbulent” viscosity:

$$\mu_{\text{effective}} = \mu + \mu_{\text{turbulent}} \quad (10)$$

The turbulent viscosity, proposed by Prandtl, is defined by Equation 11, below.

$$\mu_{\text{turb}} = \rho (\kappa y)^2 \left| \frac{\partial u}{\partial y} \right| \quad (11)$$

where,  $\rho$  = local density of the fluid,  
 $\kappa$  = Prandtl’s mixing length constant (0.4),  
 $y$  = distance from the wall,  
 $u$  = local fluid velocity parallel to the wall.

Prandtl’s formulation requires knowledge of local positioning with respect to a wall(s); however, GFSSP’s formulation (outlined earlier) is fully unstructured. In order to implement the above approach into GFSSP, either additional information is required in the input file, or a modification to the definition of “ $y$ ” in Equation 11 is needed. Based upon a desire to easily allow for an individual model to provide results for both laminar and turbulent approaches with minimal input change by the user, the latter approach of

modifying the definition of “y” was chosen. The new definition of “y” for Equation 11 is the distance between the branches, which is a required input for the laminar approach already. Therefore, for turbulent flow, Equation 4, 5, and 6 become Equations 12, 13, and 14.

$$\mu \frac{\partial^2 \mathbf{u}}{\partial y^2} V \Big|_{\text{Turbulent}} \approx \left( \mu + \left\{ \rho (\kappa \Delta y)^2 \left| \frac{\Delta \mathbf{u}}{\Delta y} \right| \right\} \right) \frac{\Delta \mathbf{u}}{\Delta y} A_{\text{shear}} \quad (12)$$

$$\mu \frac{\partial \mathbf{u}}{\partial y} A_{\text{Branch 12 shear}} \approx \left[ \left( \left\{ \mu + \left[ \rho (\kappa \cdot YN)^2 \left| \frac{u_{N12} \cos \theta_{N12} - u_{12}}{YN} \right| \right] \right\} \frac{u_{N12} \cos \theta_{N12} - u_{12}}{YN} AN \right) \right. \\ \left. + \left( \left\{ \mu + \left[ \rho (\kappa \cdot YS)^2 \left| \frac{u_{12} - u_{S12} \cos \theta_{S12}}{YS} \right| \right] \right\} \frac{u_{12} - u_{S12} \cos \theta_{S12}}{YS} AS \right) \right] \quad (13)$$

$$\mu \frac{\partial \mathbf{u}}{\partial y} A_{\text{Branch 12 shear}} \approx \sum_{i=1}^n \left( \left\{ \mu + \left[ \rho (\kappa \cdot Y_i)^2 \left| \frac{u_{i12} \cos \theta_{i12} - u_{12}}{Y_i} \right| \right] \right\} \frac{u_{i12} \cos \theta_{i12} - u_{12}}{Y_i} A_i \right) \quad (14)$$

Equation 14 represents the actual branch-branch turbulent shear formulation put into GFSSP.

### 3.3.2.2 Branch -Wall Interaction

Turbulent shear stress interaction between a solid (wall) and an adjacent branch is modeled using the log law of the wall [12]. The log law of the wall utilizes a characteristic turbulence distance from the wall ( $y^+$ ) and a characteristic velocity ( $u^+$ ).  $y^+$  is a function of wall shear stress, and  $u^+$  is a function of  $y^+$  and wall shear stress; therefore an iterative scheme is required to calculate wall shear stress. Equations 15, 16, and 17 are the three equations that are iterated upon until a converged value for wall shear stress is achieved.

$$y^+ = \frac{\rho y \left( \frac{\tau}{\rho} \right)^{\frac{1}{2}}}{\mu} \quad (15)$$

where,  $\rho$  = local fluid density  
 $\mu$  = local fluid viscosity  
 $y$  = local distance from wall

$$u^+ = \begin{cases} y^+ & \text{if } y^+ < 5.0 \\ -3.05 + 5.0(\log(y^+)) & \text{if } 5.0 \leq y^+ < 30.0 \\ 5.5 + 2.5(\log(y^+)) & \text{if } y^+ \geq 30.0 \end{cases} \quad (16)$$

$$\tau = \mu \left. \frac{\partial u}{\partial y} \right| = \rho \left( \frac{u}{u^+} \right)^2 \quad (17)$$

where,  $u$  = local velocity parallel to the wall

In order to initiate the iterative process, a seed value of the wall shear stress must be provided. The seed value of wall shear stress utilized is given by Equation 18:

$$\tau_{\text{initial guess}} = \frac{\mu u}{y} \quad (18)$$

Equations 15-18 represent the actual branch-wall turbulent shear stress formulation incorporated into GFSSP.

### 3.4 Transverse Momentum Transport

The transverse momentum component of Equation 3 can be expressed in terms of a force per unit volume.

$$\frac{\partial \rho v u}{\partial y} V \approx \frac{(\rho v \Delta u)}{(\Delta y)} (\Delta x)(\Delta y)(\Delta z) = (\Delta x)(\Delta z)(\rho v \Delta u) = m_{\text{trans, dot}} \Delta u \quad (19)$$

Figure 4 represents a set of nodes and branches for which transverse momentum exchange will take place. Let the branch 12 represent the current branch which will receive transverse momentum from the surrounding branches. Branch S12 represents an adjacent parallel branch, while branches S1 and S2 represent the adjacent normal branches.

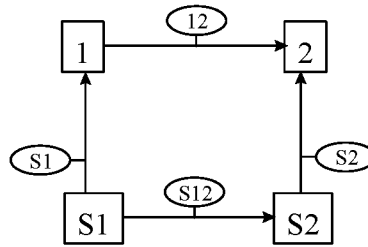


Figure 4: Branch and Node Schematic for Transverse Momentum Exchange

Now, examine the formulation for calculating the transverse momentum term for branch 12. First, calculate the average mass flow rate for the adjacent normal branches:

$$m_{S,\dot{}} = \frac{1}{2} (m_{S1,\dot{}} + m_{S2,\dot{}}) \quad (20)$$

Examining Figure 4, a positive transverse mass flow rate is defined as flow into the nodes corresponding to the branch in question. Based on this definition of transverse mass flow rate, calculate the transverse momentum term:

$$\left. \frac{\partial \rho v u}{\partial y} V \right|_{12} \approx (m_{S,\dot{}} u_{12} - m_{S,\dot{}} u_{S12}) = m_{S,\dot{}} (u_{12} - u_{S12}) \quad (21)$$

The parallel branch (S12) will contribute to the transverse momentum term of branch 12 when  $\dot{m}_{12} \geq 0$  (since a positive transverse flow rate begins at S12 and ends at 12), and should have a negligible contribution when  $\dot{m}_{12} < 0$  (i.e. transverse flow rate begins at 12 and ends at S12). Equation 22, is the upwinding representation of the transverse momentum term for branch 12.

$$\left. \frac{\partial \rho v u}{\partial y} V \right|_{12} \approx u_{12} (\max\{-m_{S,\dot{}}, 0\}) - u_{S12} (\max\{0, m_{S,\dot{}}\}) \quad (22)$$

Equation 22 can be generalized for  $m$ -parallel branches around branch  $i$ , each with an angle  $\theta_{ij}$  with respect to branch  $i$ , and  $n_{ij}$  corresponding transverse connecting branches, each transverse branch with an angle of  $\theta_{ijk}$  with respect to branch  $i$ . Equation 23 represents this generalized version of Equation 22.

$$\left. \frac{\partial \rho v u}{\partial y} V \right|_i \approx \sum_{j=1}^{m_i} \left[ u_i \left( \max \left\| - \sum_{k=1}^{n_{ij}} \left\{ \frac{1}{n_{ij}} m_{ijk,\dot{}} \cos \theta_{ijk} \right\}, 0 \right\| \right) - (u_{ij} \cos \theta_{ij}) \left( \max \left\| 0, \sum_{k=1}^{n_{ij}} \left\{ \frac{1}{n_{ij}} m_{ijk,\dot{}} \cos \theta_{ijk} \right\} \right\| \right) \right] \quad (23)$$

Equation 23 represents the actual transverse momentum formulation put into GFSSP, where  $i$  is the current branch for which transverse momentum is being calculated,  $m_i$  is the number of parallel branches which will be used to calculate transverse momentum, and  $n_{ij}$  is the number of connecting transverse branches between the current branch  $i$ , and the  $j^{\text{th}}$  parallel branch.

#### 4.0 Verification Results

In order to verify proper implementation of the shear and transverse momentum components into GFSSP, three models were identified and developed. Two verification

models were benchmarked for both laminar and turbulent flow. These two models are: two dimensional Poiseuille flow and two dimensional Couette flow. The third model was benchmarked with the laminar flow solution only. This third model is the two dimensional shear driven flow in a square cavity. The following sections describe the models and presents the results.

#### 4.1 Poiseuille Flow Model

Consider the flow between two fixed flat plates shown in Figure 5. The flow is pressure driven and assumed to be fully developed. The analytical solution for this situation can easily be derived for laminar flow. Figure 6 shows an approximate velocity profile for the laminar situation.

A simple 3 node, 10 branch model (two sets of 5 parallel branches) was constructed to model the physical situation described above. The model is shown schematically in Figure 7.

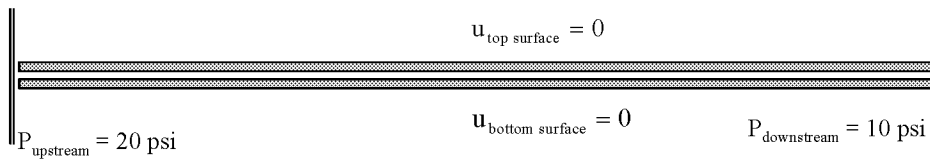


Figure 5: Poiseuille Flow Physical Situation

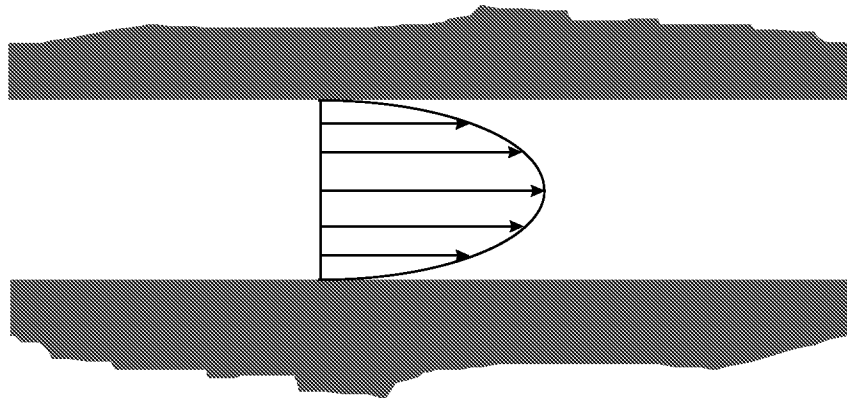


Figure 6: Poiseuille Flow Velocity Profile

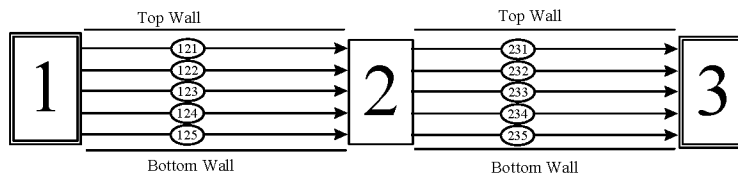


Figure 7: GFSSP Poiseuille Flow Model

The GFSSP's flow through a restriction resistance option was used in the initial flow field calculation (for the first Newton-Raphson iteration, after which the shear will replace the friction factor calculation) for each of the branches. The bottom and top walls are fixed.

Figure 8 shows a comparison between the velocity profiles for the known solutions (analytical for laminar and experimental for turbulent) and the GFSSP 3 node, 10 branch (5 parallel branch) model. As can be seen in Figure 8, the results of this crude GFSSP model compare very favorably with the analytical solution.

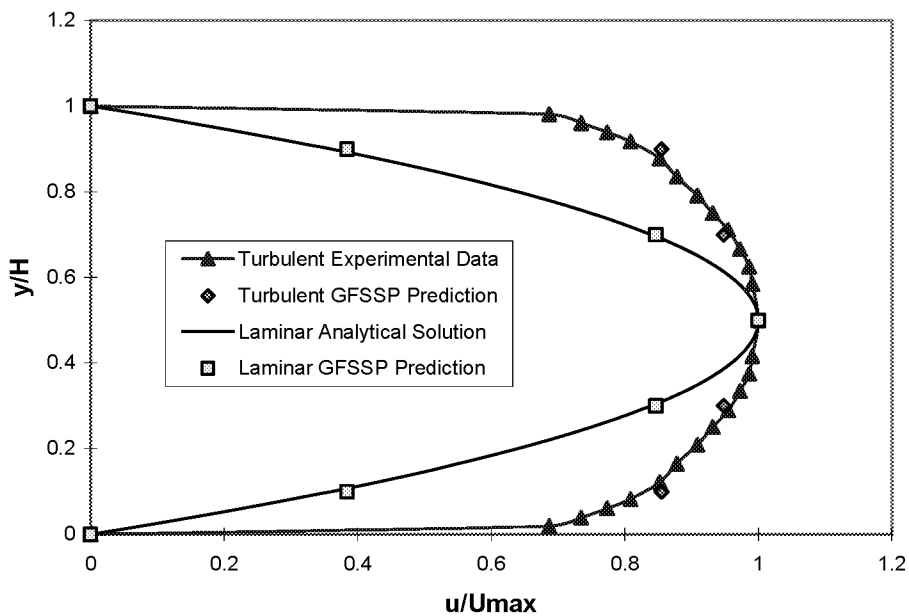


Figure 8: Poiseuille Flow Velocity Distribution

## 4.2 Couette Flow

Consider the flow between two fixed flat plates shown in Figure 9. The flow is shear driven and assumed to be fully developed. The solution to the laminar case is a linear velocity profile, illustrated in Figure 10.

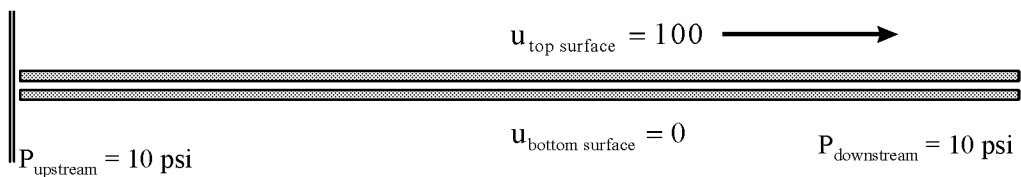


Figure 9: Couette Flow Physical Situation

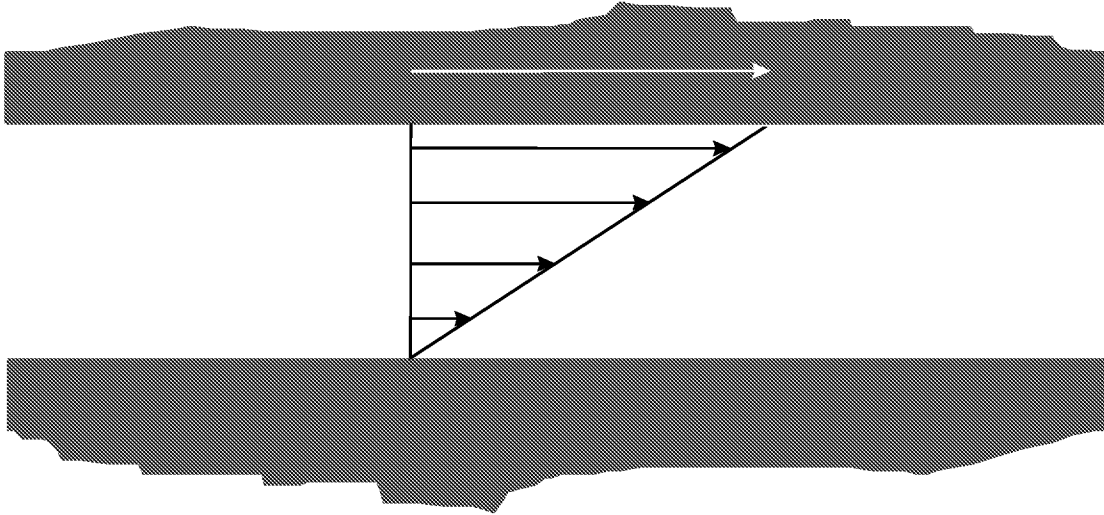


Figure 10: Laminar Couette Flow Velocity Profile

A simple 3 node, 10 branch model (two sets of 5 parallel branches) was constructed to model the physical situation. The model is shown schematically in Figure 11.

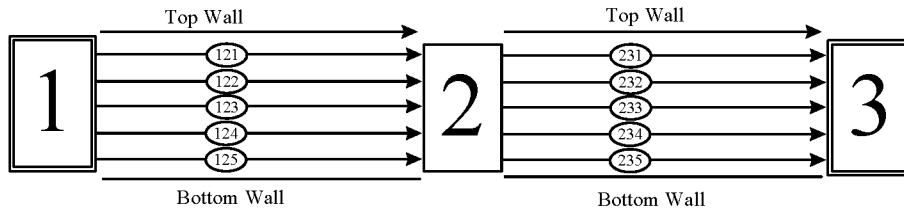


Figure 11: GFSSP Couette Flow Model

As with the Poiseuille flow case, resistance option -02 was used in the initial flow field calculation (for the first Newton-Raphson iteration, after which the shear will replace the friction factor calculation) for each of the branches. The bottom walls are fixed, and the top walls are moving at a known velocity.

Figure 12 shows the comparison between the velocity profiles for the known solutions (analytical for the laminar case, experimental results for the turbulent case) and the GFSSP 3 node, 10 branch (5 parallel branch) model. As can be seen in Figure 12, the results of this crude GFSSP model compare nearly identically with the analytical solution.

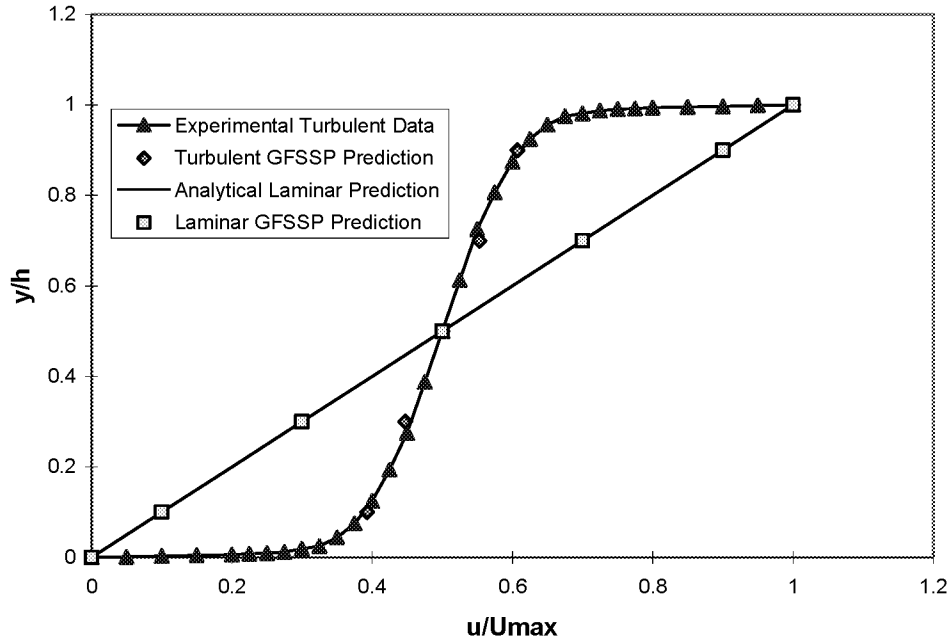


Figure 12: Couette Flow Velocity Distribution

### 4.3 Shear Driven Flow in a Square Cavity

Consider a square cavity as shown in Figure 13. The flow is induced by shear interaction at the top wall. The bottom and side walls are fixed. The top wall is moving to the right at constant speed. The corresponding Reynolds number for this situation is  $Re = 100$ .

#### 4.3.1 Benchmark Numerical Solution

Due to the non-linearity of the governing differential equations, an analytical solution of this situation is not available. Instead of an analytical solution, a well known numerical solution by Odus Burggraf [13] was used as the benchmark. Burggraf used a  $51 \times 51$  grid in his model of the square cavity.

#### 4.3.2 GFSSP Driven Cavity Model

The GFSSP model of the driven cavity consists of 49 nodes (48 of which are internal) and 84 branches.

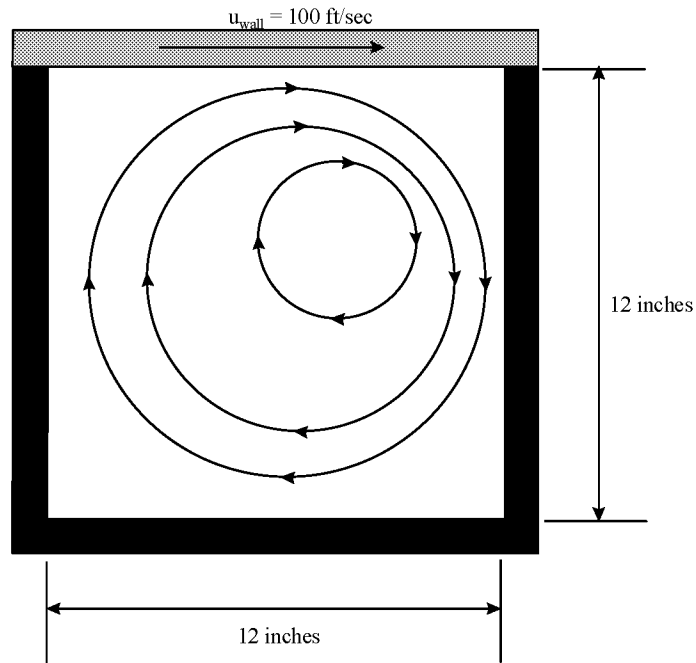


Figure 13: Flow in a Shear Driven Square Cavity

For numerical stability, one node (Node 1) was assigned to be a boundary node with an arbitrary pressure. A unit depth was assumed for the required areas. The model is shown schematically in Figure 14. As in the previous cases, GFSSP's flow through a restriction resistance Option was used in the initial flow field calculation for all of the branches. The bottom and side walls are fixed. The top walls are moving to the right at known velocity. All parallel angles are  $0^\circ$ , and all transverse angles are  $90^\circ$ .

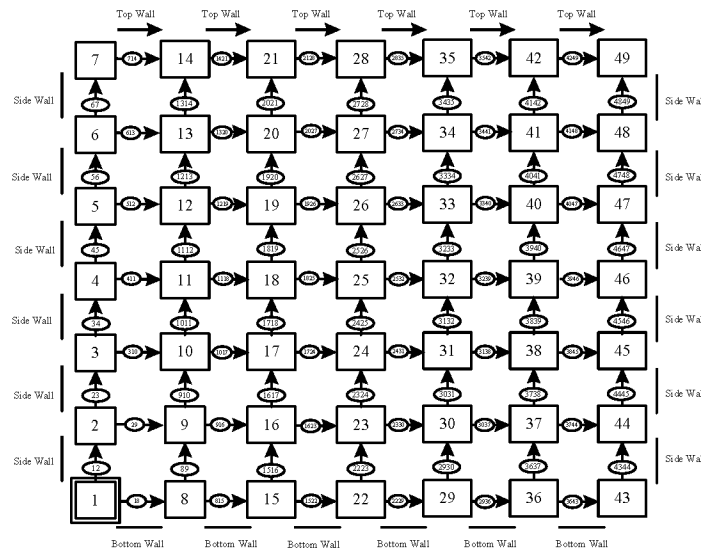


Figure 14: GFSSP Flow in a Shear Driven Square Cavity Model

### 4.3.3 Results

Figure 15 shows a comparison between the benchmark numerical solution and GFSSP 7x7 node model velocity profiles along a vertical plane at the horizontal midpoint. As can be seen in Figure 15, the results of this crude GFSSP model compare very favorably with the benchmark numerical solution of Burggraf [13].

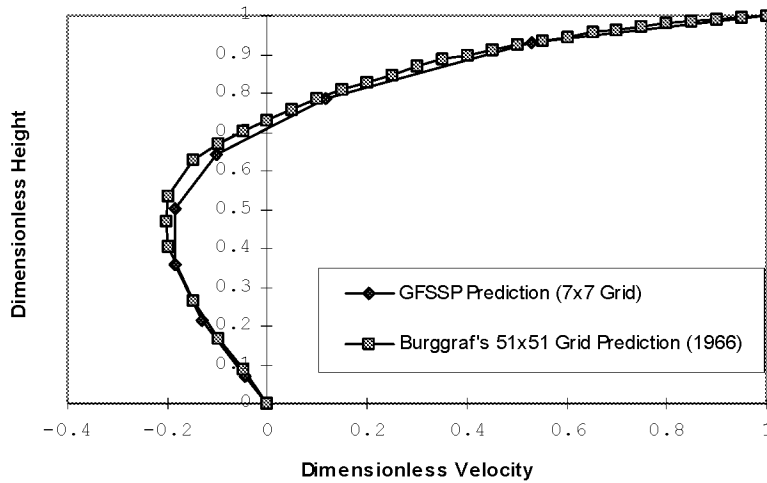


Figure 15: Shear Driven Square Cavity Centerline Velocity Distribution

## 5.0 Conclusions

This paper presents a numerical algorithm to extend a system level flow network code that was designed to solve one dimensional momentum equation to perform multi-dimensional flow calculation. The algorithm uses an identical mathematical framework for both system and component level analysis. The multi-dimensional features were incorporated by including additional momentum sources due to shear stress and transport of momentum due to transverse component of velocity. The simplicity and ease of the formulation can largely be attributed to the use of unstructured co-ordinate system. Excellent agreement with analytical solution was obtained for laminar flow in three benchmark problems: Poiseuille Flow, Couette flow and shear driven flow in a square cavity. Turbulence is modeled by an effective viscosity which is calculated from Prandtl's mixing length theory. Numerical predictions compared well with turbulent Couette flow data.

## 6.0 Acknowledgements

The work was performed at Sverdrup Technology (MSFC Group) under contract NAS8-40386, Task Directives 611-022, 550-5500-0500.

## 7.0 References

1. Majumdar, A.K.: *A Generalized Fluid System Simulation Program to Model Flow Distributions in Fluid Networks*, (User's Manual) Report No. MG-99-290, NASA MSFC Contract No. NAS 8-40836, November 1999.
2. Patankar, S., *Numerical Heat Transfer and Fluid Flow*, Hemisphere Publishing Co., New York, 1980.
3. Hendricks, R. C., Baron, A. K., and Peller, I. C., "GASP - A Computer Code for Calculating the Thermodynamic and Transport Properties for Ten Fluids: Parahydrogen, Helium, Neon, Methane, Nitrogen, Carbon Monoxide, Oxygen, Fluorine, Argon, and Carbon Dioxide", NASA TN Dd-7808, February, 1975.
4. Hendricks, R. C., Peller, I. C., and Baron, A. K., "WASP - A Flexible Fortran IV Computer Code for Calculating Water and Steam Properties", NASA TN D-7391, November, 1973.
5. Cryodata Inc., "User's Guide to GASPAK, Version 3.20", November 1994.
6. Van Hooser, Bailey John and Majumdar Alok, "Numerical Prediction of Transient Axial Thrust and Internal Flows in a Rocket Engine Turbopump", Paper No. AIAA 99-2189, 35<sup>th</sup> AIAA/ASME/SAE/ASEE Joint Propulsion Conference and Exhibit, June 21, 1999, Los Angeles, CA.
7. Holt, Kimberly, Majumdar, Alok, Steadman Todd, and Hedayat, Ali, Paper No. AIAA 2000-3719 "36<sup>th</sup> AIAA/ASME/SAE/ASEE Joint Propulsion Conference and Exhibit, July 16-19, 2000, Huntsville, AL.
8. Schallhorn, Paul, Elrod, David, Goggin, David and Majumdar, Alok, "A Fluid Circuit Model for Long Bearing Squeeze Film Damper Rotordynamics", AIAA Journal of Propulsion and Power, Vol. 16, No. 5, pp 777-780, Sept-Oct 2000.
9. Majumdar, Alok and Steadman, Todd, "Numerical Modeling of Pressurization of a Propellant Tank", AIAA Journal of Propulsion and Power, Vol. 17, No. 2, March-April 2001.
10. Cross, Matthew, F, Majumdar Alok K, Bennett, Jr., John C., and Malla, Ramesh B., "Modeling of Chill Down in Cryogenic Transfer Lines", Accepted for publication in AIAA Journal of Spacecraft and Rocket.
11. Schallhorn, P.: *Development of the Generalized Fluid System Simulation Program for Multidimensional Flow*, Sverdrup Report No. 661-022-97-003, April 1997.
12. Schlichting, H., *Boundary Layer Theory*, 6<sup>th</sup> Edition, McGraw-Hill, 1964 .
13. Burggraf, O.R.: "Analytical and Numerical Studies of the Structure of Steady Separated Flows", *Journal of Fluid Mechanics*, Vol. 24, part 1, pp. 113-151, 1966.